

Norfloxacin Zn(II)-based complexes: acid base ionization constant determination, DNA and albumin binding properties and the biological effect against *Trypanosoma cruzi*

Ligiane R. Gouvea · Darliane A. Martins · Denise da Gama Jean Batista ·
Maria de Nazaré C. Soeiro · Sonia R. W. Louro · Paulo J. S. Barbeira ·
Letícia R. Teixeira

Received: 28 March 2013 / Accepted: 11 July 2013
© Springer Science+Business Media New York 2013

Abstract Zn(II) complexes with norfloxacin (NOR) in the absence or in the presence of 1,10-phenanthroline (phen) were obtained and characterized. In both complexes, the ligand NOR was coordinated through a keto and a carboxyl oxygen. Tetrahedral and octahedral geometries were proposed for $[\text{ZnCl}_2(\text{NOR})]\cdot\text{H}_2\text{O}$ (**1**) and $[\text{ZnCl}_2(\text{NOR})(\text{phen})]\cdot 2\text{H}_2\text{O}$ (**2**), respectively. Since the biological activity of the chemicals depends on the pH value, pH titrations of the Zn(II) complexes were performed. UV spectroscopic studies of the interaction of the complexes with calf-thymus DNA (CT DNA) have suggested that they can bind to CT DNA with moderate affinity in an intercalative mode. The interactions between the Zn(II) complexes and bovine serum albumin (BSA) were investigated by steady-state and time-resolved fluorescence spectroscopy at pH 7.4. The experimental data showed static quenching of BSA fluorescence, indicating that both complexes bind to BSA. A modified Stern–Volmer

plot for the quenching by complex **2** demonstrated preferential binding near one of the two tryptophan residues of BSA. The binding constants obtained (K_b) showed that BSA had a two orders of magnitude higher affinity for complex **2** than for **1**. The results also showed that the affinity of both complexes for BSA was much higher than for DNA. This preferential interaction with protein sites could be important to their biological mechanisms of action. The analysis in vitro of the Zn(II) complexes and corresponding ligand were assayed against *Trypanosoma cruzi*, the causative agent of Chagas disease and the data showed that complex **2** was the most active against bloodstream trypomastigotes.

Keywords Norfloxacin · Zn(II) complexes · Anti-*T. cruzi* activity · Acid ionization constant · Interaction with DNA · Interaction with bovine serum albumin

L. R. Gouvea · D. A. Martins · P. J. S. Barbeira ·
L. R. Teixeira (✉)
Departamento de Química, Universidade Federal de
Minas Gerais, Belo Horizonte, MG 31270-901, Brazil
e-mail: lregina@qui.ufmg.br

D. da Gama Jean Batista · M. de Nazaré C. Soeiro
Laboratório de Biologia Celular, Instituto Oswaldo Cruz,
FIOCRUZ, Rio de Janeiro, RJ 21040-360, Brazil

S. R. W. Louro
Departamento de Física, Pontifícia Universidade Católica
do Rio de Janeiro, Rio de Janeiro, RJ 22653-900, Brazil

Introduction

Norfloxacin [1-ethyl(-6-fluoro-1,4-dihydro-4-oxo-7-(1-piperazinyl)-quinoline-3-carboxylic acid) (NOR), which was patented in 1978, is a synthetic and potent fluoroquinolone antibacterial agent for oral administration. In general, the antibacterial spectrum of NOR includes a wide variety of aerobic gram-negative and gram-positive bacteria (Appelbaum and Hunter 2000;

Emami et al. 2005; Shaikh et al. 2007; Hooper 1999). The chemical structure of NOR is shown in Fig. 1.

In the literature, there are only few references to the anti-parasitic activity of fluoroquinolones and their complexes (Martins et al. 2012; Batista et al. 2011). *Trypanosoma cruzi*, the causative agent of Chagas disease, affects more than ten million individuals in Latin America. In relation to the treatment of the disease the only current options are benznidazole and nifurtimox. Both present limited efficacy, especially, during the later chronic phase and cause undesirable secondary side effects. Thus, the identification of novel therapeutic agents more selective and presenting higher activity spectrum is an urgent need (Martins et al. 2012; Batista et al. 2011; Coura and Dias 2009; Dias 2007).

The biological activity of NOR is directly related to its ability to cross cell membranes, to bind to cytoplasmic proteins and/or inhibit the replication of DNA of the microorganism. In this sense, the coordination of metal ions to fluoroquinolones can facilitate and improve their mechanism of action (Shaikh et al. 2007).

Previous data showed that the mixed-ligand copper and manganese complexes of 1,10-phenanthroline (phen) result in higher potency against *E. coli* as compared to the free quinolone or the cupric-phen complex. The phen is a ligand with a nitrogen donor heterocycle that can increase the interaction with DNA (Yesilel et al. 2006; Arounaguiri et al. 2000).

In this context, our aim was investigate the synthesis and the structural characterization of new Zn(II) complexes with the first-generation quinolone antibacterial drug NOR in the absence or in the presence of 1,10-phen followed by the biological analysis of their potential effect in vitro against *T. cruzi*.

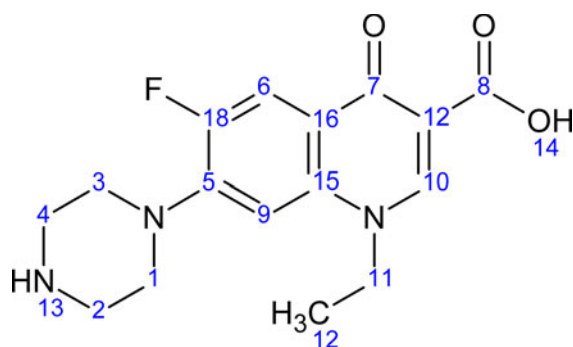


Fig. 1 Structure of norfloxacin

The coordination of a metal ion to a ligand influences the ligand's physicochemical properties. In this work, we studied the effect of the coordination in the acid base ionization constant (pK_a) (Shaikh et al. 2007; Luiz et al. 2011).

Norfloxacin has two ionizable functional groups: an acid (carboxylic group) and a basic group (amine group). In an aqueous solution, it shows three different species, which are cationic, zwitterionic and anionic. The cationic and the anionic forms predominate in acid and basic solutions, respectively. At physiological pH value (pH 7.4), the fluoroquinolone is totally or partially ionized and the predominant specie is the zwitterionic form (Shaikh et al. 2007; Luiz et al. 2011). The three relevant forms of the NOR in aqueous solution ($4 < \text{pH} < 11$) are shown in Fig. 2.

The activity of the fluoroquinolones is directly related to the pH values, since the presence of charged groups is required for biological activity. For example, the reduction in activity in lower pH values is generally attributed to the low penetration of the cationic species in the cell membrane (Shaikh et al. 2007). Consequently, we calculated the NOR-Zn(II) complexes pK_a values.

Furthermore, in order to understand the transportation, uptake and receptor binding of the Zn(II) complexes at molecular level, we also studied the interaction of the complexes with DNA and bovine serum albumin (BSA). DNA is one of the possible targets of anti-*T. cruzi* chemicals, which may include the parasites mitochondrial or nuclear DNA, while BSA is the bovine variant of the most abundant plasma protein in mammals and is responsible for the transportation of chemicals in the plasma (Martins et al. 2012; Skyrianou et al. 2010).

In order to investigate the binding properties of the complexes with calf-thymus DNA (CT DNA) UV spectroscopy was used. The affinity between Zn(II) complexes and BSA was investigated using steady-state and time-resolved fluorescence spectroscopy.

Experimental

Materials

Norfloxacin, CT DNA and BSA were purchased from Sigma-Aldrich. ZnCl_2 was purchased from Vetec. All solvents were purchased from Merck.

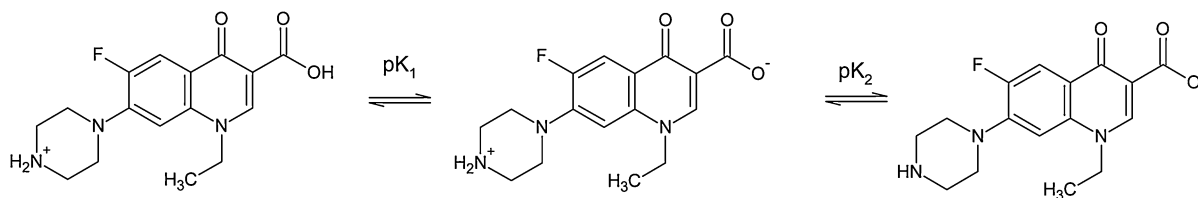


Fig. 2 Acid–base equilibria of the norfloxacin in acidic, neutral and alkaline means

The DNA stock solution was prepared by dissolving CT DNA in a universal buffer at pH 7.4 (Perrin and Dempsey 1974) followed by continuous stirring under refrigeration for 3 days, and maintained at 4 °C for no longer than a week. The stock solution of CT DNA gave a UV absorbance at 260 and 280 nm (A_{260}/A_{280}) of 1.90, indicating that the DNA was sufficiently free of protein contamination. The DNA concentration was determined by the UV absorbance at 260 nm after 1:20 dilution using $\epsilon = 6,600 \text{ L mol}^{-1} \text{ cm}^{-1}$ (Marmur 1961; Skyrianou et al. 2009).

The solutions of BSA ($2 \times 10^{-6} \text{ mol L}^{-1}$) and Zn(II) complexes were prepared in 0.1 mol L^{-1} universal buffer at pH 7.4 (Perrin and Dempsey 1974). The concentration of both Zn(II) complex solutions were $8 \times 10^{-6} \text{ mol L}^{-1}$ for both the pK_a and BSA studies and $2.5 \times 10^{-5} \text{ mol L}^{-1}$ for the DNA interaction studies.

Instrumentation—physical measurements

Elemental analyses were performed on a Perkin Elmer 2400 CHN Elemental Analyzer. The thermogravimetric curves were obtained in a Thermobalance Shimadzu TGA-5H air atmosphere (flow rate of 50 mL min^{-1}). The heating rate was 10 °C and the final temperature reached was 750 °C.

Molar conductivity measurements were taken from the Zn(II) complexes using a dimethylformamide (DMF) solution with $1 \times 10^{-3} \text{ mol L}^{-1}$ concentration. The measurements were taken using a Quimis, model Q405M, conductivity meter after calibration with a KCl aqueous solution ($k = 74.00 \mu\text{S cm}^{-1}$) as a standard solution.

Infrared (IR) spectra ($370\text{--}4,000 \text{ cm}^{-1}$) were obtained on a Mattson Instruments Galaxy, model 3000 spectrophotometer using potassium bromide (KBr) pellets. NMR spectra were obtained with a Bruker DRX-400 Avance (400 MHz) spectrometer

using d^6 -DMSO (deuterated dimethyl sulfoxide) as the solvent and tetramethylsilane as internal reference.

The pK_a measurements and DNA studies were performed on a Cary Eclipse Varian-Agilent spectrophotometer. In the BSA studies, UV–Visible absorption spectra were obtained with a diode array spectrophotometer HP 8452A (Agilent) using 1.00 cm quartz cells. Fluorescence spectra were recorded on a PTI QM1 spectrofluorometer (Photon Technology International, Birmingham, NJ). Fluorescence lifetimes were measured using an IBH-Horiba-Jobin-Yvon TCSPC system. The light source used for excitation was a 330 nm nanoLED N-16, 1.0 ns nominal pulse duration, 1 MHz repetition rate. Computer programs supplied by Horiba Jobin Ivon IBH which perform reconvolution fits were employed for processing the time decay curves. Fluorescence decay analysis of each titration set was performed with multiexponential expressions ($0.9 < \chi^2 < 1.2$).

Synthesis of the complexes

$[\text{ZnCl}_2(\text{NOR})] \cdot \text{H}_2\text{O}$ (I)

Appropriate quantities of NOR (0.25 mmol) were dissolved in acetone (40 mL), which were then added to a 5 mL acetone solution of ZnCl_2 (0.25 mmol). Immediately after the addition of the ligand, a precipitate was formed. The reaction mixture was continuously stirred at room temperature for 24 h. The solid obtained was vacuum filtered, washed with diethyl ether and dried.

$[\text{ZnCl}_2(\text{NOR})] \cdot \text{H}_2\text{O}$: yield: 86 %. Anal. calc. for $\text{C}_{16}\text{H}_{22}\text{Cl}_2\text{FN}_3\text{O}_4\text{Zn}$: C, 40.4; H, 4.7; N, 8.8. Found: C, 40.0; H, 4.4; N, 8.4 %. Conductivity ($1 \times 10^{-3} \text{ mol L}^{-1}$ in DMF): $10 \mu\text{S cm}^{-1}$. IR (cm^{-1}): 1586 s (strong) $\nu(\text{C}=\text{O})$; 1628 s $\nu_{\text{as}}(\text{COO}^-)$; 1384 s $\nu_{\text{s}}(\text{COO}^-)$; 3386 m $\nu(\text{NH})$; 2,464 and 2,772 m $\nu(\text{NH}_2^+)$. TG: mass loss (313–373 K): 4.8 % (found),

3.8 % (calc). ^1H NMR (DMSO- d_6): 1.40 (t, H-12); 2.67 (m, H2, H4); 3.23 (m, H1, H3); 4.58 (q, H11); 7.20 (d, H9); 7.95 (d, H6), 8.95 (s, H10). ^{13}C NMR (DMSO- d_6) δ : 177.13 (C7); 166.07 (C8); 151.48, 153.95 (C18); 148.65 (C10); 144.65 (C5); 137.10, 137.14 (C15); 119.75, 119.81 (C16); 111.26, 111.49 (C6); 107.13 (C12); 105.58, 106.19 (C9); 49.07 (C1, C3); 43.36 (C2, C4); 47.32 (C11); 14.42 (C12).

[ZnCl₂(NOR)(phen)]·2H₂O (2)

The precursor [ZnCl₂(phen)] was obtained using appropriate quantities of phen (0.50 mmol) dissolved in methanol (35 mL). This solution was added to a methanolic solution (5 mL) of ZnCl₂ (0.50 mmol). Immediately after the addition of phen, a precipitate was formed. The reaction mixture was stirred continuously at room temperature for 24 h. The solid obtained was vacuum filtered, washed with diethyl ether and dried.

Appropriate quantities of the precursor, [ZnCl₂(phen)], (0.25 mmol) were dissolved in acetone (20 mL), which were then added to a acetone solution (40 mL) of NOR (0.25 mmol). Immediately after the addition of the ligand, a precipitate was formed. Once again, the reaction mixture was stirred continuously at room temperature for 24 h and the solid obtained was vacuum filtered and washed with diethyl ether and dried.

[ZnCl₂(phen)]: yield: 89 %. Anal. calc. for C₁₂H₈Cl₂N₂Zn: C, 45.5; H, 2.6; N, 9.6. Found: C, 45.4; H, 2.2; N, 9.4 %. Conductivity (1×10^{-3} mol L⁻¹ in DMF): 21 $\mu\text{S cm}^{-1}$. IR (cm⁻¹): 1426 s $\nu(\text{CC, CN})$; 1519 s $\nu(\text{CC, CN})$; 853 s $\gamma(\text{CH})$; 726 s $\gamma(\text{CH})$.

[ZnCl₂(NOR)(phen)]·2H₂O (2): yield: 80 %. Anal. calc. for C₂₈H₃₁Cl₂FN₅O₅Zn: C, 49.8; H, 4.9; N, 10.4. Found: C, 49.5; H, 3.7; N, 10.3 %. Conductivity (1×10^{-3} mol L⁻¹ in DMF): 23 $\mu\text{S cm}^{-1}$. IR (cm⁻¹): 1579 s $\nu(\text{C=O})$; 1626 s $\nu_{\text{as}}(\text{COO}^-)$; 1385 s $\nu_{\text{s}}(\text{COO}^-)$, 848 m $\gamma(\text{CH})$; 728 m $\gamma(\text{CH})$; 3422 s $\nu(\text{NH})$; 2,468 and 2,732 m $\nu(\text{NH}_2^+)$. TG: mass loss (373–423 K): 4.9 % (found), 4.8 % (calc). ^1H NMR (DMSO- d_6): 1.40 (t, H-12); 3.10 (m, H2, H4); 3.43 (m, H1, H3); 4.60 (q, H11); 7.18 (d, H9); 7.90 (d, H6), 8.95 (s, H10). ^{13}C NMR (DMSO- d_6) δ : 177.11 (C7); 166.09 (C8); 151.54, 153.95 (C18); 148.51 (C10); 145.22, 145.32 (C5); 136.62, 137.15 (C15); 119.31, 119.38 (C16); 111.10, 111.34 (C6); 107.04 (C12); 105.28,

105.84 (C9); 48.84 (C1, C3); 44.22 (C2, C4); 47.32 (C11); 14.34 (C12).

Anti-*Trypanosoma cruzi* activity

Parasites

Y strain of *T. cruzi* was used throughout the experiments. Bloodstream forms were harvested by heart puncture from *T. cruzi*-infected Swiss mice at the peak of parasitemia (Meirelles et al. 1982).

Trypanocidal analysis

For the in vitro analysis on trypomastigotes, the parasites were incubated at 37 °C in the presence of increasing doses (0–200 μM) of each compound diluted in Dulbecco's modified medium supplemented with 5 % fetal bovine serum and 1 mM L-glutamine (DMES) (Batista et al. 2009). After 24 h, death rates were determined by light microscopy through the direct quantification of live parasites using a Neubauer chamber, and IC₅₀ values (drug concentration that reduces 50 % of the number of lived parasites) were then calculated as reported (Daliry et al. 2009).

pK_a determination of the norfloxacin and the Zn(II) complexes

The Henderson–Hasselbalch equation describes the derivation of pH as a measure of acidity, using pK_a , the negative log of the acid dissociation constant, in biological and chemical systems (Luiz et al. 2011).

In order to determine the pK_a values it was necessary to know the concentration of protonated and neutral species in solution, depending on the pH. These concentrations were obtained by emission spectroscopy. The spectroscopic parameter used was the fluorescence intensity at a given wavelength, I_λ . The equation below (Luiz et al. 2011) gives I_λ as a function of the pH, for one titration site:

$$I_\lambda = \frac{I_{\lambda 1}10^{pK} + I_{\lambda 2}10^{pH}}{10^{pH} + 10^{pK}} \quad (1)$$

where $I_{\lambda 1}$ and $I_{\lambda 2}$ are the fluorescence intensity of the protonated and deprotonated drug, respectively, at a given wavelength. In the case of two titratable groups the equation is:

$$I_{\lambda} = \frac{I_{\lambda 1} 10^{pK_1}}{10^{pH} + 10^{pK_1}} + \frac{I_{\lambda 2} 10^{pH}}{10^{pH} + 10^{pK_1}} \cdot \frac{10^{pK_2}}{10^{pH} + 10^{pK_2}} + \frac{I_{\lambda 3} 10^{pH}}{10^{pH} + 10^{pK_2}} \quad (2)$$

where $I_{\lambda 1}$, $I_{\lambda 2}$ and $I_{\lambda 3}$ are the fluorescence intensities of the lowest, intermediate and highest pH form of the drug, respectively, at a given wavelength.

DNA binding studies

The interaction of Zn(II) complexes with CT DNA were studied with UV spectroscopy in order to investigate the possible binding modes to CT DNA and to calculate the binding constants (K_b). Binding constants, K_b , were determined using a constant concentration of the complexes recorded in the absence or presence of increasing CT DNA amounts. K_b values were obtained by monitoring the changes in the absorbance of the complexes at 272 and 271 wavelengths for complexes **1** and **2**, respectively. K_b was given by the ratio of the slope to the y-intercept in plots of $[DNA]/(\epsilon_a - \epsilon_f)$ versus $[DNA]$, according to the Eq. (3) (Pyle et al. 1989):

$$\frac{[DNA]}{\epsilon_a - \epsilon_f} = \frac{[DNA]}{\epsilon_b - \epsilon_f} + \frac{1}{[K_b(\epsilon_b - \epsilon_f)]} \quad (3)$$

where $[DNA]$ is the concentration of DNA in base pairs, ϵ_a , ϵ_f and ϵ_b corresponds to the apparent extinction coefficient $A_{\text{obsd}}/[\text{compound}]$, the extinction coefficient for the free compound, and the extinction coefficient for the compound in the fully bound form, respectively.

Bovine serum albumin (BSA) binding studies

The protein-binding studies were performed by tryptophan fluorescence quenching experiments using BSA ($2 \mu\text{mol L}^{-1}$) dissolved in a phosphate buffer at pH 7.4. The quenching of the emission intensity at 338 nm of BSA tryptophan residues (Trp-134, Trp-213) was monitored using increasing amounts of complexes **1** and **2** as quenchers. Fluorescence spectra were recorded from 300 to 500 nm at an excitation wavelength of 285 nm. The fluorescence spectra of the quenchers (complexes **1** and **2**) in the buffer solution were recorded under the same experimental conditions and exhibited a

maximum emission of 412 nm. Therefore, the quantitative studies of the serum albumin fluorescence spectra were performed after correction by subtracting the spectra of the complexes.

Stern–Volmer analysis is useful in the estimation of the accessibility of tryptophan residues in proteins to the drug molecules (quenchers) and was used to study the interaction between the quenchers and bovine serum albumin. According to the Stern–Volmer equation for dynamic quenching, Eq. (4) (Lakowicz and Weber 1973):

$$\frac{F_0}{F} = 1 + k_q \tau_0 [Q] + K_{SV} [Q] \quad (4)$$

where F_0 and F are the steady-state fluorescence intensities in the absence and presence of the quencher, respectively. k_q is the bimolecular quenching rate constant of BSA, τ_0 is the average lifetime of BSA without the quencher, $[Q]$ is the concentration of the quencher. K_{SV} is the Stern–Volmer quenching constant. According to Eq. (4), the relation between K_{SV} and k_q in case of dynamic quenching is (Lakowicz and Weber 1973)

$$K_{SV} = k_q \tau_0 \quad (5)$$

but in the case of static quenching, due to the formation of a ground-state non-fluorescent complex, K_{SV} is the actual association constant of the quencher with the protein.

Results and discussion

Microanalysis and molar conductivity studies

Microanalysis suggested the formation of $[\text{ZnCl}_2(\text{NOR})] \cdot \text{H}_2\text{O}$ (**1**) and $[\text{ZnCl}_2(\text{NOR})(\text{-phen})] \cdot 2\text{H}_2\text{O}$ (**2**) in which NOR is the NOR ligand and phen is the 1,10-phen co-ligand. The thermogravimetric data confirmed the presence of hydration water molecules in the complexes' structures. The neutrality of the compounds was revealed by the conductivity data in a 1:1 DMF solution. The values obtained, between 10 and $23 \Omega^{-1} \text{cm}^2 \text{mol}^{-1}$, were well below the conductivity level generally associated with a 1:1 electrolyte in DMF (between 65 and $90 \Omega^{-1} \text{cm}^2 \text{mol}^{-1}$), according to the literature, suggesting a non-electrolyte covalent feature (Geary 1971).

Infrared spectral studies

The IR spectrum of free NOR exhibited one band at $1,617\text{ cm}^{-1}$, which was assigned to the stretching vibration of $\nu(\text{CO})_{\text{ketonic}}$. In the spectra of the complexes, the $\nu(\text{CO})$ was affected by the interaction with the metal ion and appeared as a shoulder around $1,579$ and $1,586\text{ cm}^{-1}$. Such behavior has been observed in several quinolone metal ion complexes (Dorofeev 2004).

The band around $1,630\text{ cm}^{-1}$ in the spectra of the complexes was assigned to the asymmetric stretching vibration (ν_{as}) of the coordinated carboxylate group. The two complexes also showed other strong intensity bands at $1,384$ and $1,385\text{ cm}^{-1}$ which were absent in the NOR spectrum and were assigned to the symmetric vibration (ν_{s}) of the coordinated COO^- group. These bands appeared after the ionization of the carboxyl group and were characterized by the formation of a resonance structure. This occurrence suggested the involvement of this group in the interaction with the metal ion (Dorofeev 2004; Gao et al. 1995; Sadeek 2005; Batista et al. 2011).

The carboxylate group can act as unidentate, bidentate or as a bridging ligand, and the frequency separation [$\Delta\nu = \nu_{\text{as}}(\text{COO}^-) - \nu_{\text{s}}(\text{COO}^-)$] between the asymmetric and symmetric stretching of this group was used to distinguish between these binding states (Sadeek 2005; Batista et al. 2011). Deacon and Phillips (1980) investigated the asymmetric and symmetric stretching vibrations of a large number of carboxylate complexes with a known crystal structure. They found that unidentate carboxylate complexes exhibit $\Delta\nu > 200\text{ cm}^{-1}$. The observed $\Delta\nu$ values were 244 and 241 cm^{-1} for complexes **1** and **2**, respectively, which suggested a unidentate interaction of the carboxylate group.

The IR spectral data of the Zn(II) complexes show a very strong broad band of about $3,400\text{ cm}^{-1}$ and medium weak to weak bands of about $2,800$ and $2,500\text{ cm}^{-1}$. These bands were assigned to the vibrations of the quaternized nitrogen in the piperazinyl group, which indicated that the zwitterionic form of NOR is involved in the coordination with the Zn(II) (Refat et al. 2010; Refat 2007).

UV–Vis absorption studies

The formation of the Zn(II) complexes was also investigated using UV–Vis spectra. Electronic spectra

of the NOR and their Zn(II) complexes were recorded in the $260\text{--}800\text{ nm}$ region in the universal buffer, pH 7.4. The absorption spectrum of the free NOR showed three bands at 272 , 324 and 334 nm , attributed to $\pi \rightarrow \pi^*$ and $n \rightarrow \pi^*$ transitions. In the spectra of the complexes, these bands showed less absorption (hypochromism), indicating that the carboxylic group and the ketone group were involved in the complexation (Refat et al. 2010; Refat 2007).

^1H NMR measurements

The ^1H NMR spectra of the free NOR present a triplet at $\delta 1.41$ attributed to CH_3 and two multiplets at $\delta 2.89$ and $\delta 3.23$ corresponding to the piperazine ring's hydrogens. The quartet corresponding to the non-aromatic CH_2 was observed at $\delta 4.56$. The signals of the aromatic hydrogens were observed at $\delta 7.13$, $\delta 7.88$ and $\delta 8.92$. In the ^1H NMR spectra of the complexes, the chemical shift values were only slightly changed, being of the order of 0.2 ppm . This subtle change was expected as there was no hydrogen near the coordination sites.

In the ^1H NMR spectra of complex **1**, a small signal at $\delta 5.73$ attributed to NH_2^+ was observed. This was due to the NOR zwitterionic form and can be observed only when the metallic ion is coordinated to the ketonic and the carboxylic carbons (Refat 2007). Owing to low solubility of complex **2**, this signal could not be observed.

^{13}C NMR measurements

The ^{13}C NMR spectra of free NOR presented signals at $\delta 176$ and $\delta 154$ attributable to the ketonic and the carboxylic carbons, respectively. The signals of the aromatic carbons were observed in the $\delta 100\text{--}\delta 152$ region. The signals corresponding to the piperazine ring carbons C2, C4 and C1, C3 were observed in about $\delta 45$ and $\delta 51$, respectively.

In the ^{13}C NMR spectra of the complexes, the chemical shift values of the piperazine ring and the aromatic carbons were only slightly changed, being in the order of $1\text{--}2\text{ ppm}$. In contrast, the signals of the ketonic and the carboxylic carbons were observed at $\delta 177$ and $\delta 166$, and showed major changes in the order of $10\text{--}12\text{ ppm}$, suggesting that Zn(II) was coordinated to the oxygens.

Normally, zinc complexes have tetrahedral or octahedral geometry (Dudev and Lim 2000). Taking

this into consideration and all data obtained, tetrahedral and octahedral geometries were proposed for $[\text{ZnCl}_2(\text{NOR})]\cdot\text{H}_2\text{O}$ and $[\text{ZnCl}_2(\text{NOR})(\text{phen})]\cdot 2\text{H}_2\text{O}$, respectively.

Fluorescence studies of NOR and their Zn(II) complexes

In the literature, the fluorescence of NOR has been reported as a function of the pH (Luiz et al. 2011). In this work, the NOR and their Zn(II) complexes spectra in aqueous solutions were obtained and compared in a pH range from 4 to 11.

At $\text{pH} > 10$, NOR showed almost no fluorescence, indicating that for high pH values it had become a non-fluorescent molecular species. When the pH decreased, the fluorescence increased, and its maximum intensity with peak at 408 nm was registered at $\text{pH} 7.6$. This transition between $\text{pH} 10$ and 7.6 is due to protonation of the distal amine of the piperazine group. In the pH range from 7.6 to 4.0 , there was a transition between two fluorescent species. The fluorescence peak at 408 nm decreased and that at 446 nm increased with decreasing pH in this range. This transition refers to the protonation of the carboxylate group (Fig. 3).

The emission spectra of Zn(II) complexes were similar over the whole pH range. Figure 4 shows the graphs of fluorescence intensities of NOR and their complexes at the two wavelengths of maximum variations, (a) 400 nm and (b) 450 nm, as a function of pH.

To determine the pK values (Fig. 4), the data were fitted by means of Eq. (2). These values appear in the legends of Fig. 4 and were observed to be the same for NOR and the two complexes. The pK_1 value obtained for the carboxylic group was 6.18 ± 0.03 . This pK_1 value referred to the transition from the zwitterionic (at neutral pH) to the cationic species (in acid pH). For the basic group, the pK_2 value obtained was 8.66 ± 0.06 . These pK_2 values referred to the transition in the alkaline range, from zwitterionic (at neutral pH) to anionic species (in basic pH). It is important to note that pK values of 6.1 and 8.6 have been previously found for both transitions of NOR (Luiz et al. 2011).

There are negligible differences in the pK values among NOR and complexes 1 and 2. Park et al. (2002) presented the formation constant (K_f) of the NOR

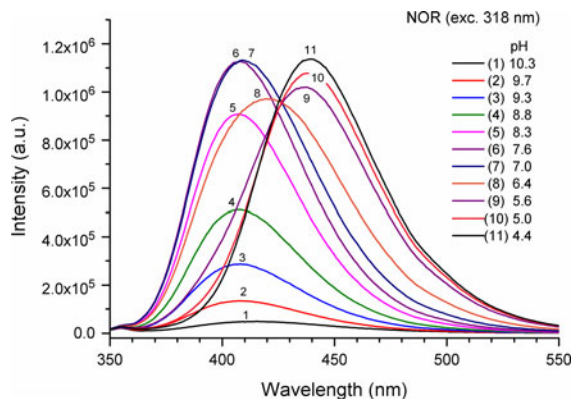


Fig. 3 Fluorescence spectra of NOR, in an aqueous solution, at different pH values. $[\text{NOR}] = 8 \times 10^{-6} \text{ mol L}^{-1}$, $\lambda_{\text{excitation}} = 318 \text{ nm}$

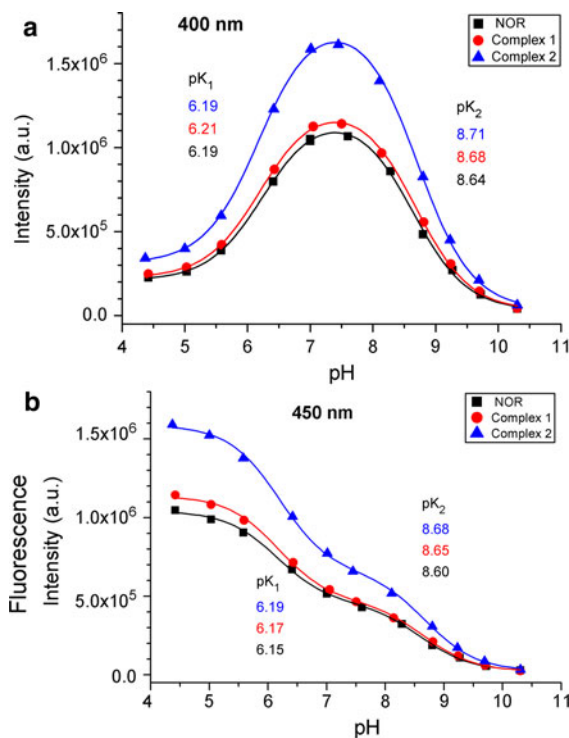


Fig. 4 Fluorescence intensities at wavelengths of maximal variations **a** 400 nm and **b** 450 nm, as function of pH, for NOR and complexes 1 and 2. The curves show the transition between the cationic–zwitterionic (pK_1) and zwitterionic–anionic (pK_2) species. Solid lines are the best fits using Eq. (2)

complexes with Zn(II) and several other metals, at physiological pH. The value obtained for Zn(II)–NOR was $7.9 \times 10^3 \text{ L mol}^{-1}$. Using this value of K_f it was possible to calculate the expected pK_1 shift, under the

assumption that Zn(II) competes with H⁺ for the carboxylic acid site. The expression for competitive interactions is (Hulme and Trevethick 2010):

$$K_{1\text{ app}} = K_1(1 + [\text{Zn}]/K_{d\text{ Zn}}) \quad (6)$$

where K_1 and $K_{1\text{ app}}$ are the real and apparent dissociation constant of the NOR carboxylic acid radical and $K_{d\text{ Zn}}$ is the dissociation constant of Zn(II). Then

$$\begin{aligned} \log(K_{1\text{ app}}/K_1) &= \log(1 + [\text{Zn}]/K_{d\text{ Zn}}) \\ \rightarrow \text{p}K_1 - \text{p}K_{1\text{ app}} &= \log(1 + [\text{Zn}]/K_{d\text{ Zn}}) \end{aligned} \quad (7)$$

Substituting $1/K_f$ for $K_{d\text{ n}}$ and $[\text{Zn}] = 8 \times 10^{-6} \text{ mol L}^{-1}$, a pK shift of 0.027 was obtained, which was negligible, and explained the results of pH titrations.

Next, the interaction of the complexes with DNA and BSA was evaluated since DNA may be a potential target of anti-*T. cruzi* drugs, which may include both mitochondrial and/or nuclear DNA (Soeiro and Castro 2011). On the other hand, as this protozoan has a blood stage which is relevant for mammalian infection (Bloodstream trypanomastigotes) and novel blood bank therapies are largely desirable (Silva et al. 2012), the potential binding of the Zn(II) complexes with the BSA was considered since it is one of the most abundant plasma protein in mammals and is responsible for the blood transportation of chemicals (Martins et al. 2012; Skyrianou et al. 2010).

Interaction with DNA

Transition metal complexes can bind to DNA via covalent and/or non-covalent interactions. In non-covalent interactions, DNA can provide three distinct binding sites for quinolone metal complexes (groove binding, electrostatic binding to phosphate group and intercalation). Electronic absorption spectroscopy is normally used to examine the binding modes of DNA with metal complexes (Cox et al. 2009).

The absorption spectra of the interaction of CT DNA with Zn(II) complexes (Fig. 5) were recorded to calculate the binding constants to CT DNA (K_b). The intensity of the bands of complexes **1** and **2** at 272 and 271 nm, respectively, in the presence of CT DNA exhibited a considerable hypochromism.

The binding constants, K_b , of Zn(II) complexes to DNA were calculated from Eq. (2). The calculated K_b values are given in Table 1 and suggested a moderate binding of the Zn(II) complexes to CT DNA. The K_b values of both Zn(II) complexes were similar. The addition of phen did not significantly change the constant values. The hypochromic effect observed might have been due to the interaction between the aromatic chromophore (from norfloxacinato ligand) of the complexes and DNA base pairs consistent with the intercalative binding mode (Cox et al. 2009; Skyrianou et al. 2009).

Interaction with BSA

As above briefly reported, BSA acts on the transport of metal ions and metal drug complexes in the human

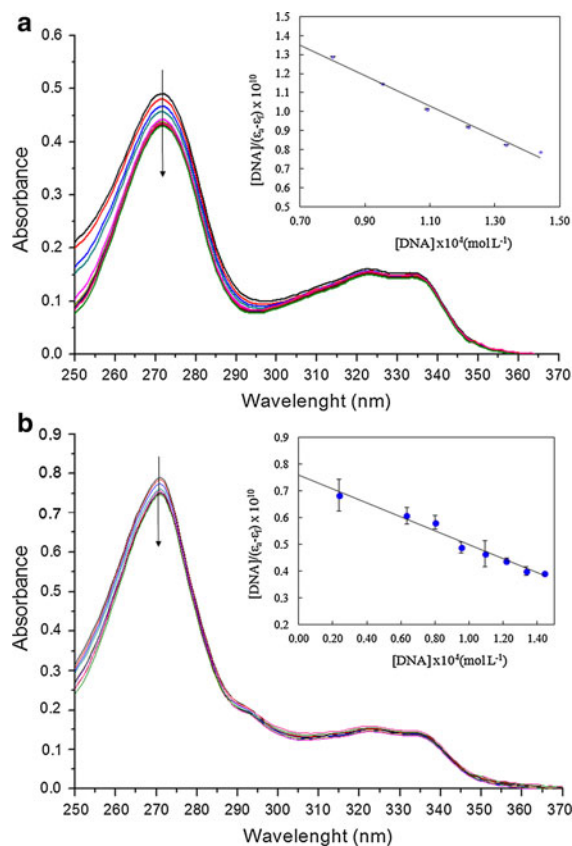


Fig. 5 UV-Vis spectra of **a** $[\text{ZnCl}_2(\text{NOR})]\cdot\text{H}_2\text{O}$, **b** $[\text{ZnCl}_2(\text{NOR})(\text{phen})]\cdot 2\text{H}_2\text{O}$ with increasing amounts of CT DNA. The arrows show the changes upon increasing amounts of CT DNA. $[\text{Compound}] = 2.5 \times 10^{-5} \text{ mol L}^{-1}$ at pH 7.4. Insets plots of $[\text{DNA}]/(\epsilon_a - \epsilon_f)$ versus $[\text{DNA}]$ at **a** 272 nm, **b** 271 nm

body. BSA, is the most extensively studied serum protein, and has two tryptophan residues, Trp-134 and Trp-212, embedded in the sub-domain IB and sub-domain IIA, respectively (Kamat 2005; Dhar et al. 2005). In this section, the interaction of two Zn(II) complexes with BSA was studied using tryptophan fluorescence-quenching experiments.

The BSA solution exhibited a strong fluorescence emission with a peak at 338 nm due to the tryptophan residues (excited at 285 nm). Figure 6 shows the fluorescence spectra of BSA in the presence of increasing amounts of the Zn(II) complexes. The addition of Zn(II) complexes to BSA resulted in a significant fluorescence quenching at 338 nm, and the appearance of an emission peak at longer wavelengths. Since the emission spectrum of Trp residues overlaps with the absorption spectrum of NOR, resonance energy transfer (RET) may have occurred. To evaluate if the development of the emission peak of the complexes comes from RET or from a direct excitation, the fluorescence spectra of the complexes were obtained under the same experimental conditions, but in the absence of BSA. The results are also presented in Fig. 6 (spectra peaked at 412 nm). It could be observed that direct excitation explained the growth of the fluorescence peak from the complex. This became more evident when subtracting the spectra of the pure complexes from the corresponding spectra in the presence of BSA and led to the fluorescence contribution of Trp, as observed in Fig. 7. The inset in Fig. 7 shows Stern–Volmer plots for the quenching of Trp fluorescence. In this plot, the fluorescence at 338 nm was corrected for the inner filter effect, according to the Eq. (8) (Lakowicz and Weber 1973).

$$F = F_{obs}10^{A_{exc}/2}. \quad (8)$$

where F_{obs} is the observed fluorescence at 338 nm, and A_{exc} is the absorbance at 285 nm.

Linear Stern–Volmer plots may either indicate the existence of a single type of quenching, or reveal the occurrence of just one binding site for the quencher in the proximity of the fluorophore. As static quenching does not require diffusion through the medium, the

quenching is more efficient and the observed quenching constant is higher. If dynamic quenching occurs, the approximate bimolecular quenching constant (k_q , $L \text{ mol}^{-1} \text{ s}^{-1}$) may be calculated from Eq. (3) taking the average fluorescence lifetime (τ_0) of tryptophan in BSA around 10^{-8} s. In the case of static quenching, the binding constant is the Stern–Volmer constant itself (Skyrianou et al. 2009).

The calculated value of K_{SV} for the interaction of complex 1 with BSA is given in Table 2 indicating good binding. In case of dynamic quenching, the bimolecular quenching constant k_q depends on the probability of a collision between fluorophore and quencher and are a measure of the exposure of tryptophan residues to the drug. The upper limit of k_q expected for a diffusion-controlled bimolecular process is $10^{10} L \text{ mol}^{-1} \text{ s}^{-1}$. The magnitude of k_q for complex 1 was in the order of $10^{13} L \text{ mol}^{-1} \text{ s}^{-1}$, which was much greater than this upper limit. For this reason, the process could not be diffusion controlled, and specific drug-protein interactions were involved (Wang et al. 2007).

It is important to mention that the obtained binding constants were related to binding sites near the Trp residues. We can not exclude the existence of other binding sites, which do not modify the intrinsic BSA fluorescence.

When a protein contains several Trp residues that are in distinct environments, each residue usually has different accessibilities to quenchers. The fluorescence of accessible Trp residues decreases in the presence of a quencher, whereas the buried residues are not quenched. Downward curvature of Stern–Volmer plots is expected if some tryptophan residues are not accessible to quenchers (Lakowicz and Weber 1973). This was the case of quenching by complex 2. The inset in Fig. 7 shows that complex 2 interacted preferentially with only one Trp residue.

A modified Stern–Volmer plot can be used to analyze differing accessibilities of tryptophan residues in proteins (Wang et al. 2007). When examining two populations of fluorophores, one of which is accessible to quenchers (a) and the other being buried (b), the Stern–Volmer equation becomes

Table 1 The DNA binding constants (K_b) obtained for the Zn(II) complexes

Compounds	K_b ($10^3 L \text{ mol}^{-1}$)	R^{2a}	Hypochromism (%)
[ZnCl ₂ (NOR)]·H ₂ O (1)	(4.45 ± 0.05)	0.9866	12
[ZnCl ₂ (NOR)(phen)]·2H ₂ O (2)	(3.5 ± 0.1)	0.9731	6

^a Linear regression

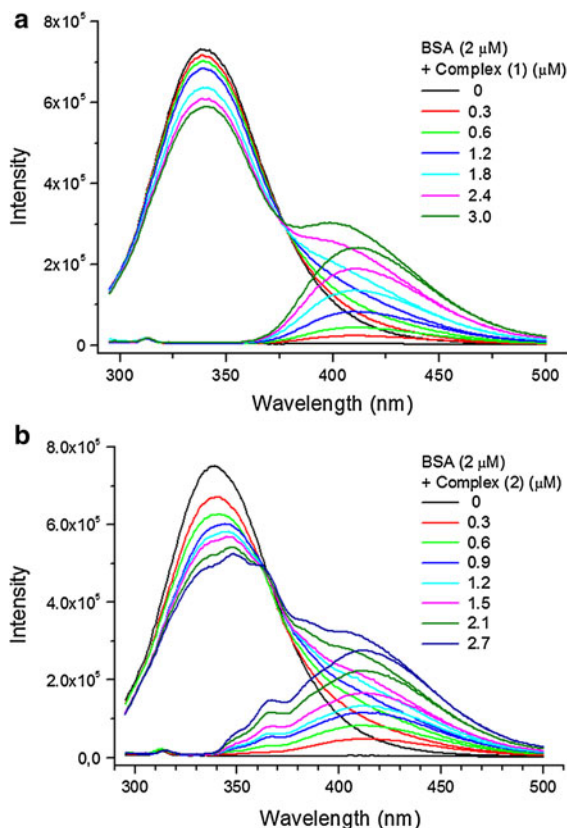


Fig. 6 Fluorescence spectra of BSA ($2 \mu\text{mol L}^{-1}$) in the presence of increasing amounts of **a** $[\text{ZnCl}_2(\text{NOR})]\cdot\text{H}_2\text{O}$ (**1**) and **b** $[\text{ZnCl}_2(\text{NOR})(\text{phen})]\cdot 2\text{H}_2\text{O}$ (**2**). $[\text{Complex}] = 8 \times 10^{-6} \text{ mol L}^{-1}$ at pH 7.4

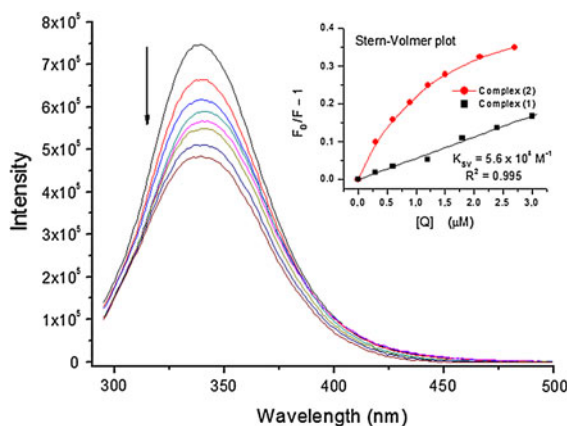


Fig. 7 Subtractions of the fluorescence spectra in Fig. 6b (BSA + complex **2** – pure complex **2**). Inset Stern–Volmer plots obtained from the fluorescence at 338 nm, for the quenching with complexes **1** and **2**

Table 2 Binding constants K_b (equal to the Stern–Volmer constants, K_{SV}) obtained for the interaction between the Zn(II) complexes and BSA

Compounds	K_{SV} (L mol^{-1})	R^{2a}
$[\text{ZnCl}_2(\text{NOR})]\cdot\text{H}_2\text{O}$ (1)	5.6×10^4	0.99
$[\text{ZnCl}_2(\text{NOR})(\text{phen})]\cdot 2\text{H}_2\text{O}$ (2)	1.2×10^6	0.99

^a Linear regression

$$\frac{F_0}{F_0 - F} = \frac{1}{f_a} + \frac{1}{f_a K_a [Q]} \quad (9)$$

where f_a is the fraction of the initial fluorescence that is accessible to quencher and K_a is the Stern–Volmer quenching constant of the accessible fraction, F_0 is the total fluorescence in the absence of quencher, and $[Q]$ is the concentration of quencher. A plot of $F_0/\Delta F$ versus $1/[Q]$ allows f_a and K_a to be determined [f_a^{-1} is the intercept and $(f_a K_a)^{-1}$ the slope]. Figure 8 presents the modified plot for quenching by complex **2**. A linear fit gave $f_a = 0.33$ and $K_a = 1.24 \times 10^6 \text{ L mol}^{-1}$.

Fluorescence lifetimes

Fluorescence decay curves for the BSA samples in the absence and presence of different concentrations of complexes **1** and **2** were obtained. Figure 9 shows the typical decay curves. These curves exhibited a small decrease in the average fluorescence lifetime with the increasing concentration of quenchers, as observed by the slope in the logarithmic plot. The curves were first analyzed individually using a three exponential expression.

$$I(t) = A + \sum_{i=1}^3 \alpha_i \exp(t/\tau_i) \quad (10)$$

It was observed that the three obtained lifetimes were very similar for all the decay curves, and the fractional contribution for each lifetime varied. This was in accordance with the mechanism of static quenching, which does not change the lifetimes. It was also observed that the contribution of the shorter lifetime ($<1 \text{ ns}$) was smaller ($<6\%$). Therefore another approach was used: the mean lifetimes with the greatest contribution were calculated $\langle\tau_1\rangle = 7.03 \text{ ns}$ and $\langle\tau_2\rangle = 3.62 \text{ ns}$. Then a global analysis

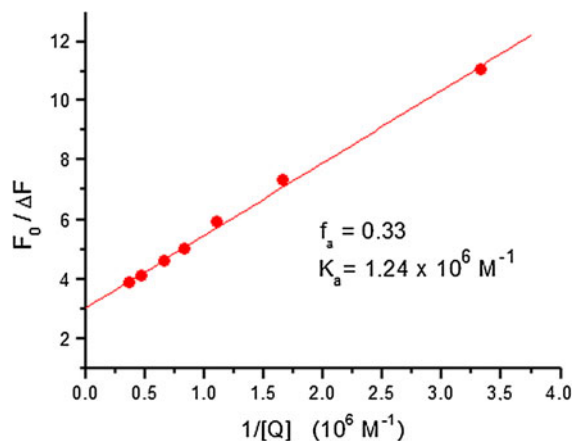


Fig. 8 Modified Stern–Volmer plot for the fluorescence quenching data obtained with complex **2** (BSA fluorescence intensity at 338 nm)

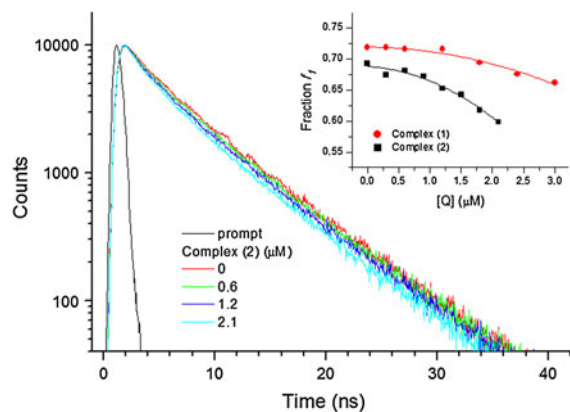


Fig. 9 Fluorescence decay curves for BSA (excitation at 282 nm, emission at 338 nm) at different concentrations of complex **2**. *Inset* fractional contribution of the longest lifetime as a function of the of the complexes concentration

was performed using all the decay curves for each quencher, **1** and **2**. The global analysis yielded the lifetimes that fit all the data and gives the fractional contributions of the lifetimes for each decay. In this global analysis the two principal lifetimes were fixed at the calculated average values above. The third lifetime τ_3 and the pre-exponential factor α_i were the fitting parameters: $\tau_1 = 7.03$ ns (fixed) and $\tau_2 = 3.62$ ns (fixed), and $\tau_3 = 0.51$ ns for complex **1** or $\tau_3 = 0.78$ ns for complex **2**. The inset of Fig. 9 depicts the fractional contribution (f_1) of τ_1 normalized to the contributions of the two main lifetimes as a function of quencher concentration, according to Eq.

(11). (The contribution of τ_3 was random and less significant because of the width of the light pulse).

$$f_1 = \frac{\alpha_1 \tau_1}{\alpha_1 \tau_1 + \alpha_2 \tau_1} \quad (11)$$

The contribution of the longest lifetime decreases slightly with increasing complex concentrations, and this can be explained by the different accessibility of the two BSA Trp residues.

Anti-*Trypanosoma cruzi* activity

Finally, the biological effect of the studied compounds was investigated in vitro. Table 3 shows the effect of all the compounds and of benznidazole (Bz), the reference drug, against bloodstream trypomastigotes forms of *T. cruzi* (Y strain) expressed as IC_{50} values.

Free NOR exerted a low trypanocidal effect against the bloodstream trypomastigote form. The association of Zn(II) with NOR in the complex **1** did not increase trypanocidal activity (Table 3).

The introduction of 1,10-phen as co-ligand was shown to be an effective strategy for improving the activity. In fact, the complex **2** was 16 times more active than the analogous without the phen and exhibited IC_{50} value of $12 \mu\text{mol L}^{-1}$, comparable to benznidazole activity, the reference drug for Chagas disease. Although the free phen and its precursor, $[\text{ZnCl}_2(\text{phen})]$, showed significant activity, the addition of a hydrophobic moiety could decreased the polarity of the compound and changed the solubility, thus helping transportation throughout the body (Arounaguir et al. 2000; Saha 2004).

Table 3 Activity (mean \pm SD) of the compounds and of benznidazole (Bz) upon bloodstream trypomastigotes (BT) forms of *T. cruzi* (Y strain), in vitro (24 h of incubation at 37 °C)

Compounds	IC_{50} ($\mu\text{mol L}^{-1}$)
Norfloracin (NOR)	127 ± 30
1,10-phenantroline (phen)	11 ± 3
ZnCl_2	>250
$[\text{ZnCl}_2(\text{NOR})] \cdot \text{H}_2\text{O}$ (1)	197 ± 75
$[\text{ZnCl}_2(\text{phen})]$	14 ± 2
$[\text{ZnCl}_2(\text{NOR})(\text{phen})] \cdot 2\text{H}_2\text{O}$ (2)	12 ± 2
Benznidazole (Bz)	13 ± 2

Conclusion

In this work, two new Zn(II) complexes with the antibacterial drug NOR were synthesized: the single ligand $[\text{ZnCl}_2(\text{NOR})]\cdot\text{H}_2\text{O}$ and mixed-ligand $[\text{ZnCl}_2(\text{NOR})(\text{phen})]\cdot 2\text{H}_2\text{O}$.

The biological activity of complexes **1** and **2** was directly related to the acid ionization constant (pK). Drugs with pK outside the 6–8 range can be ionized and poorly absorbed through the cell membrane (Patrick 1995). Using fluorescence spectroscopy, pK values of the acidic group (carboxylic group), pK_1 , and the basic group (amine group), pK_2 , of these compounds were obtained. The differences were negligible. This was explained by a formation constant of the order of 10^4 L mol^{-1} (Park et al. 2002).

Spectrophotometric studies showed that the complexes interact with DNA with binding constants in the order of 10^3 L mol^{-1} , which characterized moderate affinity. The K_b values of Zn(II) complexes were similar, and the presence of phen did not change significantly the affinity. The observed hypochromism probably appeared as a consequence of the intercalative binding mode and is due to $\pi \rightarrow \pi^*$ stacking interactions in DNA (Pyle et al. 1989).

Interaction of the complexes with BSA was studied using fluorescence. The fluorescence of the complexes did not change in the presence of BSA. However, the strong fluorescence emission of BSA due to the two tryptophan residues was quenched by the complexes. RET from Trp residues to NOR was not observed. Static quenching allowed obtaining the BSA binding constants for the two complexes. Complex **2** preferentially quenches one the Trp residues. As the Trp-134 is located on the protein surface, its fluorescence is more easily suppressed by complex **2**. On the other hand the Trp-212 is located in a hydrophobic cavity which has a more difficult access (Lakowicz 2004). The presence of phen in the complex increased the affinity for BSA by a factor of 20.

Finally, our present results related to the efficacy of the Zn(II) complexes with NOR showed that a considerable increase in the levels of parasite lyses was achieved with complex **2**. Due to the lack of successful therapy for several neglected diseases including Chagas disease, the synthesis and screening of new candidates still represents a relevant challenge justifying the current analysis and furthers studies in this line of investigation.

Acknowledgments The present study was supported by Fundação de Amparo a Pesquisa do Estado de Minas Gerais (FAPEMIG), Fundação de Amparo a Pesquisa do Estado do Rio de Janeiro (FAPERJ), Conselho Nacional de Desenvolvimento Científico e Tecnológico (CNPq) and PDTIS/Fiocruz.

References

- Appelbaum PC, Hunter PA (2000) The fluoroquinolones: past, present and future perspectives. *Int J Antimicrob Agents* 16:5–15
- Arounaguiri S, Easwaramoorthy D, Ashokkumar A, Dattagupta A, Maiya BG (2000) Cobalt(III), nickel(II) and ruthenium(II) complexes of 1,10-phenanthroline family of ligands: DNA binding and photocleavage studies. *Proc Indian Acad Sci* 112:1–17
- Batista DGJ da, Silva PB da, Stivanin L, Lachter DR, Silva RS, Felcman J, Louro SRW, Teixeira LR, Soeiro M de NC (2011) Co(II), Mn(II) and Cu(II) complexes of fluoroquinolones: synthesis, spectroscopical studies and biological evaluation against *Trypanosoma cruzi*. *Polyhedron* 30:1718–1725
- Batista DGJ, Pacheco MGO, Kumar A, Branowska D, Ismail MA, Hu L, Boykin DW, Soeiro MNC (2009) Biological, ultrastructural effect and subcellular localization of aromatic diamidines in *Trypanosoma cruzi*. *Parasitology* 137:251–259
- Batista DGJ, Silva PB, Garcia LS, Lachter DR, Silva RS, Felcman J, Louro SRW, Teixeira LR, Soeiro MNC (2011) Co(II), Mn(II) and Cu(II) complexes of fluoroquinolones: synthesis, spectroscopical studies and biological evaluation against *Trypanosoma cruzi*. *Polyhedron* 30:1718–1725
- Coura JR, Dias JC (2009) Epidemiology, control and surveillance of Chagas disease: 100 years after its discovery. *Mem Inst Oswaldo Cruz* 104:31–40
- Cox PJ, Psomas G, Bolos CA (2009) Characterization and DNA-interaction studies of 1,1-dicyano-2,2-ethylene dithiolate Ni(II) mixed-ligand complexes with 2-amino-5-methyl thiazole, 2-amino-2-thiazoline and imidazole. Crystal structure of $[\text{Ni}(\text{i-MNT})(2\text{-a-5mt})(2)]$. *Bioorg Med Chem* 17:6054–6062
- Daliry A, da Silva PB, da Silva CF, Batista MM, de Castro SL, Tidwell RR, Soeiro MNC (2009) In vitro analyses of the effect of aromatic diamidines upon *Trypanosoma cruzi*. *J Antimicrob Chemother* 64:747–750
- Deacon GB, Phillips RJ (1980) Relationships between the carbon–oxygen stretching frequencies of carboxylato complexes and the type of carboxylate coordination. *Coord Chem Rev* 33:227–250
- Dhar S, Nethaji M, Chakravarty AR (2005) Effect of charge transfer bands on the photo-induced DNA cleavage activity of [1-(2-thiazolylazo)-2-naphtholato]copper(II) complexes. *J Inorg Biochem* 99:805–812
- Dias JC (2007) Southern cone Initiative for the elimination of domestic populations of *Triatoma infestans* and the interruption of transfusional Chagas disease. Historical aspects, present situation and perspectives. *Mem Inst Oswaldo Cruz* 102:11–18
- Dorofeev VL (2004) Infrared spectra and the structure of drugs of the fluoroquinolone group. *Pharm Chem J* 38:693–697

- Dudev T, Lim C (2000) Tetrahedral vs. octahedral Zn^{2+} complexes with ligands of biological interest: a DFT/CDM study. *J Am Chem Soc* 122:11146–11153
- Emami S, Shafiee A, Foroumadi A (2005) Quinolones: recent structural and clinical developments. *Iran J Pharm Res* 3:123–136
- Gao F, Yang P, Xie J, Wang H (1995) Synthesis, characterization and antibacterial activity of novel Fe(III), Co(II), and Zn(II) complexes with norfloxacin. *J Inorg Biochem* 60:61–67
- Geary WJ (1971) The use of conductivity measurements in organic solvents for the characterization of coordination compounds. *Coord Chem Rev* 7:81–122
- Hooper DC (1999) Mechanisms of fluoroquinolone resistance. *Drug Resist Updates* 2:38–55
- Hulme EC, Trevethick MA (2010) Ligand binding assays at equilibrium: validation and interpretation. *Br J Pharmacol* 161:1219–1237
- Kamat BP (2005) Study of the interaction between fluoroquinolones and bovine serum albumin. *J Pharm Biomed Anal* 39:1046–1050
- Lakowicz JR (2004) Principles of fluorescence spectroscopy, 2nd edn. Springer, New York
- Lakowicz JR, Weber G (1973) Quenching of fluorescence by oxygen: probe for structural fluctuations in macromolecules. *Biochemistry* 12:4161–4170
- Luiz FCL, Garcia LS, Goes Filho LS, Teixeira LR, Louro SRW (2011) Fluorescence studies of gold(III)–norfloxacin complexes in aqueous solutions. *J Fluoresc* 21:1933–1940
- Marmur J (1961) A procedure for the isolation of deoxyribonucleic acid from microorganisms. *J Mol Biol* 3:208–218
- Martins DA, Gouvea LR, Gama JBD da, Silva PB da, Louro SR, Soeiro M de NC, Teixeira LR (2012) Copper(II)–fluoroquinolone complexes with anti-*Trypanosoma cruzi* activity and DNA binding ability. *BioMetals* 25:951–960
- Meirelles MN, de Araujo-Jorge TC, de Souza W (1982) Interaction of *Trypanosoma cruzi* with macrophages in vitro: dissociation of the attachment and internalization phases by low temperature and cytochalasin B. *Z Parasitenkd* 68:7–14
- Park H-R, Kim TH, Bar K-M (2002) Physicochemical properties of quinolone antibiotics in various environments. *Eur J Med Chem* 37:443–460
- Patrick GL (1995) An introduction to medicinal chemistry. Oxford University Press, New York
- Perrin DD, Dempsey B (1974) Buffers for pH and metal ion control. Chapman and Hall, New York
- Pyle AM, Rehmann JP, Meshoyrer R, Kumar CV, Turro NJ, Barton JK (1989) Mixed-ligand complexes of ruthenium(II): factors governing binding to DNA. *J Am Chem Soc* 111:3051–3058
- Refat MS (2007) Synthesis and characterization of norfloxacin-transition metal complexes (group 11, IB): spectroscopic, thermal, kinetic measurements and biological activity. *Spectrochim Acta A* 68:1393–1405
- Refat MS, Mohamed GG, de Farias RF, Powell AK, El-Garib MS, El-Korashy SA, Hussien MA (2010) Spectroscopic, thermal and kinetic studies of coordination compounds of Zn(II), Cd(II) and Hg(II) with norfloxacin. *J Therm Anal Calorim* 102:225–232
- Sadeek SA (2005) Synthesis, thermogravimetric analysis, infrared, electronic and mass spectra of Mn(II), Co(II) and Fe(III) norfloxacin complexes. *J Mol Struct* 753:1–12
- Saha DK (2004) A novel mixed-ligand antimycobacterial dimeric copper complex of ciprofloxacin and phenanthroline. *Bioorg Med Chem Lett* 14:3027–3032
- Shaikh AR, Giridhar R, Yadav MR (2007) Bismuth–norfloxacin complex: synthesis, physicochemical and antimicrobial evaluation. *Int J Pharm* 332:24–30
- Silva CF, Batista DG, Oliveira GM, Souza EM, Hamer ER, da Silva PB, Daliry A, Araujo JS, Brito C, Rodrigues ACM, Liu Z, Farahat AA, Kumar A, Boykin D, Blader I, Soeiro MNC (2012) *In vitro* and *in vivo* investigation of the efficacy of arylimidamide DB1831 and its mesylated salt form—DB1965—against *Trypanosoma cruzi* infection. *PLoS One* 7:30356
- Skyrianou KC, Efthimiadou EK, Psycharis V, Terzis A, Kessissoglou DP, Psomas G (2009) Nickel–quinolones interaction. Part 1—nickel(II) complexes with the antibacterial drug sparfloxacin: structure and biological properties. *J Inorg Biochem* 103:1617–1625
- Skyrianou KC, Perdih F, Turel I, Kessissoglou DP, Psomas G (2010) Nickel–quinolones interaction. Part 3—nickel(II) complexes of the antibacterial drug flumequine. *J Inorg Biochem* 104:740–749
- Soeiro MNC de, Castro SL de (2011) Screening of potential anti-*Trypanosoma cruzi* candidates: *in vitro* and *in vivo* studies. *Open Med Chem J* 5:21–30
- Wang Y, Zhang H, Zhang G, Tao W, Tang S (2007) Interaction of the flavonoid hesperidin with bovine serum albumin: a fluorescence quenching study. *J Lumin* 126:211–218
- Yesilel OZ, Soyulu MS, Olmez H, Buyukgungor O (2006) Synthesis and spectrothermal studies of vitamin B13 complexes of cobalt(II) and nickel(II) with 4-methylimidazole: crystal structure of $[Ni(HOr)(H_2O)(4-Meim)_3]_2 \cdot 5H_2O$. *Polyhedron* 25:2985–2992